

Spinal effects of acupuncture stimulation assessed by proton density-weighted functional magnetic resonance imaging at 0.2 T

Geng Li^{a,*}, Man Cheuk Ng^{a,b}, Kelvin K. Wong^a, Keith D. Luk^b, Edward S. Yang^a

^a*The Jockey Club MRI Center, The University of Hong Kong, Pokfulam, Hong Kong*

^b*Department of Orthopedics and Traumatology, Faculty of Medicine, The University of Hong Kong, Pokfulam, Hong Kong*

Received 6 June 2005; revised 15 October 2005; accepted 15 October 2005

Abstract

Signal changes can be detected by proton density-weighted functional imaging in both the brain and the spinal cord. These are attributed to changes in extravascular water proton (signal enhancement by extravascular protons) density during neuronal activation. In this study, we used this technique to detect correlations between acupoint stimulation and neural activity in the spinal cord. Stimulation of acupoints associated with treatment of sensorimotor deficits (LI4 and LI11) was performed on 11 volunteers. During stimulation, 8 of the 11 subjects had consistent functional activations in C6/C7. A bilateral activation pattern was common. Our findings show that acupoint stimulation modulates activity in the spinal cord.

© 2005 Elsevier Inc. All rights reserved.

Keywords: Acupoints; BOLD; Neural pathway; SEEP; Spinal cord

1. Introduction

Functional brain activation is seen in proton density-weighted spin-echo functional magnetic resonance imaging (fMRI) [1]. This signal enhancement by extravascular protons (SEEP) [2] was proposed to appear along with blood oxygenation level-dependent (BOLD) signals during functional activation. Various experiments have been carried out to verify this new contrast mechanism [3–8]. One of such verification studies performed low-field proton density-weighted fMRI studies on the brain [4]. Because the fractional signal variation due to the change in extravascular proton density is independent of the field whereas the BOLD effect diminishes to a negligible level with short echo times in a low magnetic field, activation detected under such conditions is mainly due to the effect of increased proton density [3].

Our group has shown that activation can be detected in the spinal cord by proton density-weighted fMRI with sensorimotor stimulation [7,8]. Other groups have also shown that this is a reliable tool for the study of neuronal activity and injury [9–11] and is useful in investigating functional activation in the human spinal cord.

The present study aims to reveal the functional activation induced by acupoint stimulation in a low-field MRI system using proton density-weighted fMRI. Acupoint stimulation at LI4 and LI11 was given to healthy subjects using a block-design paradigm. Acupoints LI4 and LI11 are treatment acupoints for upper limb numbness according to the acupuncture literature [12]. We refer to these as sensorimotor-implicated acupoints. We performed a current in-depth qualitative and quantitative study on the activation area and the fractional signal change in the spinal cord using a proton density-weighted sequence at 0.2 T. This study is the first attempt to investigate the effect of acupoint stimulation in the cervical spinal cord. Preliminary results have been reported in conference publications [13,14].

2. Methods

fMRI studies were carried out on 28 healthy volunteers (age = 25.96 ± 5.25 years; 14 males) with a 0.2-T Profile MRI System (General Electric Medical System, Milwaukee, WI, USA) following a protocol approved by the ethics committee of the QiaoTou Hospital (Dong Guan, Guangzhou, China). Each subject gave fully informed consent prior to participating in the experiment. All subjects included in the current study were aged between 20 and 36 years,

* Corresponding author. Tel.: +852 2293 0305; fax: +852 2540 6215.



Fig. 1. Stimulation paradigm. R indicates rest; A, acupoint stimulation.

right-handed and had normal cervical spinal cords without a history of myelopathy, trauma or other spinal diseases/injuries. For screening, sagittal T2-weighted and axial T1-weighted images were acquired for each subject before the fMRI study to exclude subjects who could not comply fully with the criteria.

Subjects were asked to lie supine, and a 9-in. GP coil was used to image the neck region from spinal levels C5/C7 to T1. Acupoint activation was achieved by simultaneous electrical stimulation at the sensory acupoints LI4 and LI11 on the left side. LI4 is located at the midpoint of the line bisecting the angle between the first and the second

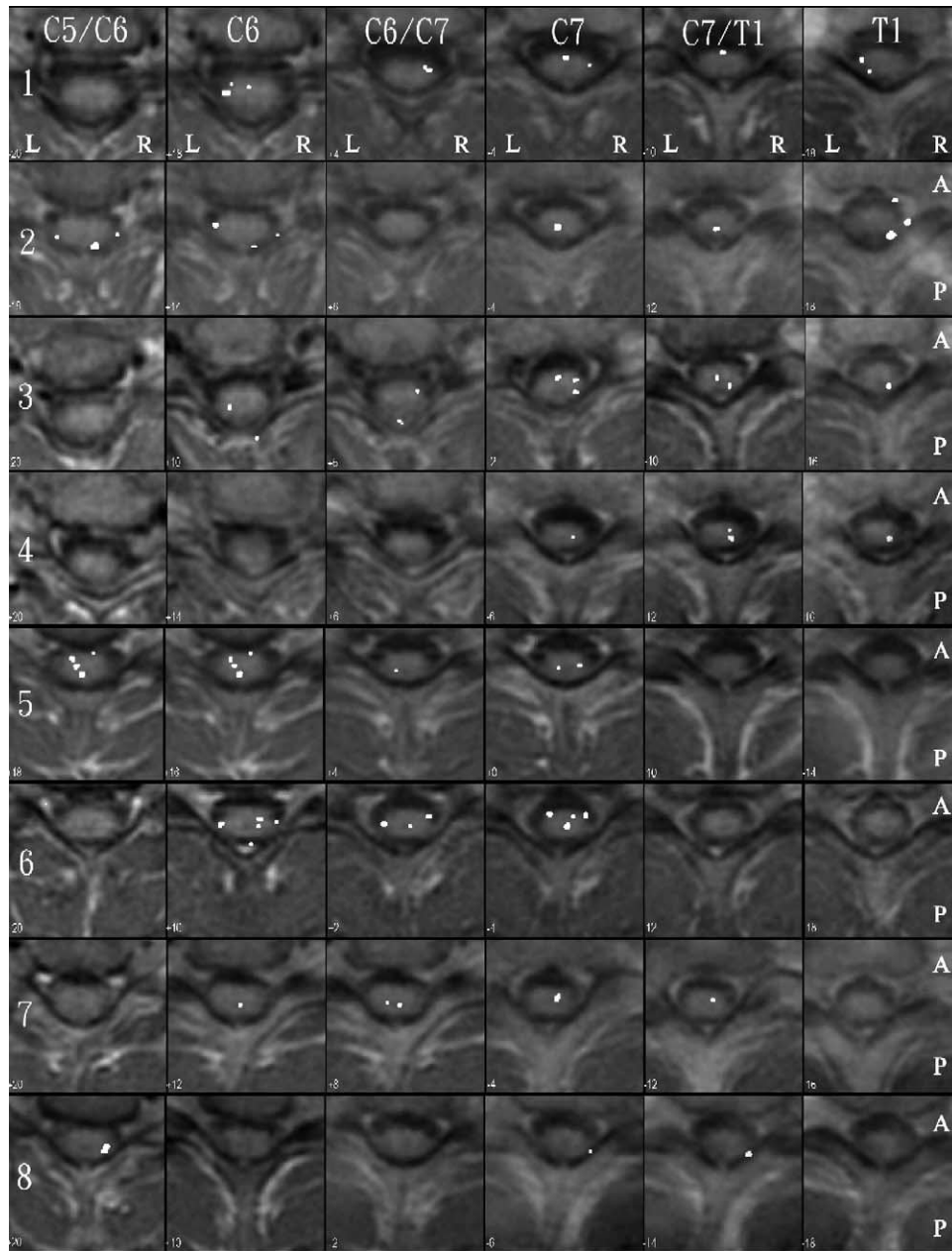


Fig. 2. Activation maps of the eight subjects with positive activation falling within the spinal cord. Each row represents one subject and each column represents one spinal level from C5/C6 to T1. The white patches in the spinal cord show the activation areas detected. L indicates left; R, right; A, anterior; and P, posterior.

metacarpal bones when the thumb is fully extended, whereas LI11 is located at the end of the lateral transverse elbow crease when the forearm is flexed at a right angle to the upper arm [12]. The initial location of acupoints was based on anatomical landmarks, proportional measurement and specific postures. The accurate location of acupoints was confirmed using an acupoint detector (Pointer Plus, Model PD-3332, Plenty Source Development, Hong Kong). Bipolar electroacupuncture at 2 Hz was conducted with the positive electrode over LI4 and the negative electrode over LI11 (Electronic Acupunctoscope, Model WQ-6F, Donghua Electronic Instrument Factory, Beijing, China) [15–18]. The intensity was set to midway between barely perceptible and maximally tolerable levels [19,20]. Subjects felt heaviness, pressure, soreness, distention, tension and numbness with the characteristic “de qi” effect [12,21,22]. A block design was used with the stimulation paradigm shown in Fig. 1. The paradigm consisted of four cycles of alternating rest and stimulation periods, with three scans (57 s/scan) during each rest period and four scans during each stimulation period. Proton density-weighted images were acquired with a fast spin-echo sequence with the following parameters: repetition time=1 s, echo time=24 ms, echo train length=6, field of view=160 mm, slice thickness=10 mm, slice spacing=1 mm, number of slices=5, matrix size=128×128, number of averages=2 and flow compensation=ON.

The data were processed offline. A rigid-body registration package, Automated Image Registration [23], was used to register the data volumes to the first scan to correct for bulk motion of the spinal cord during the scans. An image mask was used in the image registration process to mask off the pharynx and neck muscles so as to yield better results. After image registration, six motion parameters, three translations and three rotations, determined from the rigid-body model were generated for each subject. Subjects with a maximum translation of >4.2 mm or with a maximum rotation of >0.04 radian in any of the three orthogonal directions during the acquisition process were excluded from analysis. The exclusion threshold values for the motion parameters were set prior to fMRI analysis to minimize bias. The total number of subjects satisfying this criterion was 11 (aged=23.9±3.8 years; 5 males). All data volumes were then resliced to a voxel size of 0.625×0.625×1.2 mm³. The resliced data sets were then analyzed using Statistical Parametric Map (SPM) 99. A box-car function was used to model the hemodynamic response. Postprocessing of fMRI data was performed using Matlab software (Version 6.1, Math Works, Natick, MA, USA) and the SPM software package (Wellcome Department of Cognitive Neurology, Institute of Neurology, Queen Square, UK). Statistical maps, SPM{t}, which were masked and overlaid on the original axial images for analysis [25], were generated for all subjects ($P < .006$). To investigate the change in MR signal intensity, we quantitatively analyzed the time course of the activation voxels falling within the mask. The mean fractional signal change induced by the proton density

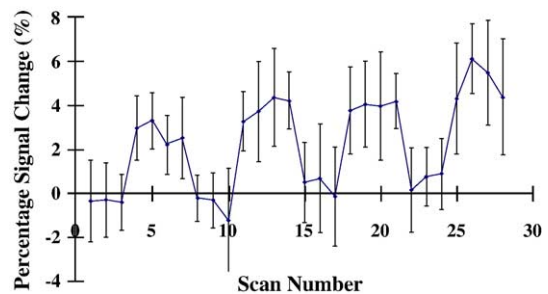


Fig. 3. Average signal change of the eight subjects' activation in the spinal cord during acupoint stimulation.

increase during the acupoint stimulation task was computed for all activated voxels within the spinal cord.

3. Results

Of the 11 included subjects, 8 (72.7%) showed positive activation in the gray matter of the spinal cord (Fig. 2). Discrete activation was found in the anterior, posterior and lateral gray horns. The activation was localized at spinal levels from T1 to C7, with peak activity at C7. The average signal change over the eight subjects was approximately 4% (Fig. 3). To detect common and focal areas of activation across subjects, we divided the spinal cords into three regions— anterior, middle and posterior. These three regions exhibited more or less the same level of activation among subjects. The proton density change was detected bilaterally in the cervical spinal cord sensorimotor areas.

4. Discussion

fMRI is a useful method for noninvasive functional brain mapping during acupoint stimulation given its relatively high temporal and spatial resolution [14–17,21,22,26–28]. Unlike most previous studies, ours first used SEEP spinal fMRI to study neuronal activation in the spinal cord during acupoint stimulation. fMRI of the human spinal cord has also been used to reveal areas of neuronal activity in response to external stimuli in both healthy and injured people [1,3,5,9,29–32]. To our knowledge, spinal cord activation as detected by fMRI during acupoint stimulation has not been previously reported.

During stimulation of acupoints LI4 and LI11, we observed a positive spread of activation across spinal cord segments from T1 to C5, with peak activity at the C7 level. This is consistent with stimulation of the median and ulnar nerves. Stimulation of the LI11 acupoint excites the lateral antibrachial cutaneous nerve. Despite the effects of motion, we were able to detect consistent areas of motor and sensory activity that correspond well with spinal cord neuroanatomy. The proton density change was detected in the cervical spinal cord sensorimotor areas bilaterally. In general, with an acupoint stimulus applied to the left hand, the activity was expected to be primarily on the left side of the cord in

the dorsal and ventral horns of the gray matter, with a spread of activity to adjacent segments and some contralateral spread. The positive activations in the anterior, middle and posterior cord were not focused in the same area because the median nerve has two roots from the lateral (C5, C6, C7) and medial (C8, T1) cords, which embrace the third part of the axillary artery, uniting anterior or lateral to it. Some fibers from C7 often leave the lateral root in the lower part of the axilla, passing distomedially posterior to the medial root, usually anterior to axillary artery, to join the ulnar nerve; they may branch from the seventh cervical ventral ramus. Also, the median nerve entering the forearm varies among individuals [24].

According to traditional Chinese medicine, acupoints LI4 and LI11 are the most important points related to sensorimotor deficits [12]. Stimulation of these acupoints may benefit patients with sensorimotor deficits by activating the spinal cord. This initial study demonstrates that SEEP spinal fMRI can be used to reliably assess activity in the cervical spinal cord during stimulation of upper limb acupoints associated with treatment of sensorimotor deficits.

5. Conclusions

In the current study, proton density-weighted fMRI using a low-field system successfully demonstrated human cervical spinal cord activity associated with acupoint stimulation. From our results, >72.7% of the subjects showed activation localized at C6/C7, corresponding to the area associated with upper limb sensorimotor deficits. Activation was detected in both the dorsal and ventral parts of the cord, which correlates with known functional neuroanatomy. The average percentage signal change was 4%. Our findings show that acupoints are regions sensitive to needle stimulation that have an ability to modulate the activity in specific spinal cord regions.

Acknowledgments

This study was partially supported by the Jockey Club Charity Trust. We thank Dr. Iain Bruce for reviewing the manuscript.

References

- [1] Stroman PW, Krause V, Malisza KL, Frankenstein UN, Tomanek B. Characterization of contrast changes in functional MRI of the human spinal cord at 1.5 T. *Magn Reson Imaging* 2001;19(6):833–8.
- [2] Stroman PW, Tomanek B, Krause V, Frankenstein UN, Malisza KL. Functional magnetic resonance imaging of the human brain based on signal enhancement by extravascular protons (SEEP fMRI). *Magn Reson Med* 2003;49(3):433–9.
- [3] Stroman PW, Krause V, Malisza KL, Frankenstein UN, Tomanek B. Extravascular proton-density changes as a non-BOLD component of contrast in fMRI of the human spinal cord. *Magn Reson Med* 2002;48(1):122–7.
- [4] Stroman PW, Malisza KL, Onu M. Functional magnetic resonance imaging at 0.2 Tesla. *Neuroimage* 2003;20(2):1210–4.
- [5] Stroman PW. Characterization of the proton-density change contribution to spin-echo fMRI data: the SEEP contrast mechanism. In *Proceedings of the 13th Annual Meeting of ISMRM*. Miami, USA; 2005. p. 118.
- [6] Stroman PW, Krause V, Frankenstein UN, Malisza KL, Tomanek B. Spin-echo versus gradient-echo fMRI with short echo times. *Magn Reson Imaging* 2001;19(6):827–31.
- [7] Ng MC, Wong KK, Li G, Ma QY, Yang ES, Hu Y, et al. Verification of proton density change in spinal cord fMRI. In the 4th IASTED International Conference on VIIP. Marbella, Spain; 2004. p. 926–30.
- [8] Wong KK, Ng MC, Hu Y, Luk KD, Ma QY, Yang ES. Functional MRI of the spinal cord at low field. In *Proceedings of 12th Annual Meeting of ISMRM*. Kyoto, Japan; 2004. p. 1534.
- [9] Stroman PW, Kornelsen J, Bergman A, Krause V, Ethans K, Malisza KL, et al. Noninvasive assessment of the injured human spinal cord by means of functional magnetic resonance imaging. *Spinal Cord* 2004; 42(2):59–66.
- [10] Stroman PW, Tomanek B, Krause V, Frankenstein UN, Malisza KL. Mapping of neuronal function in the healthy and injured human spinal cord with spinal fMRI. *Neuroimage* 2002;17(4):1854–60.
- [11] Bergman AD, LeBlanc C, Stroman PW. Spinal fMRI of multiple sclerosis: comparison of signal intensity changes with healthy controls. In *Proceedings of 12th Annual Meeting of ISMRM*. Kyoto; 2004. p. 1035.
- [12] Stux GPB. *Basics of acupuncture*. Berlin: Springer; 1998.
- [13] Wong KK, Ng MC, Li G, Hu Y, Luk KD, Yang ES. Proton density-weighted spinal fMRI comparison between sensorimotor task and acupoint stimulation. In *Proceedings of the 13th Annual Meeting of ISMRM*. Miami, USA; 2005. p. 1465.
- [14] Li G, Wong K, Ng M, Hu Y, Luk K, Yang E. Proton density change in spinal cord fMRI induced by acupoint stimulation. *Proc Int Soc Magn Reson Med* 2005;13:1095.
- [15] Li G, Liu HL, Cheung RT, Hung YC, Wong KK, Shen GG, et al. An fMRI study comparing brain activation between word generation and electrical stimulation of language-implicated acupoints. *Hum Brain Mapp* 2003;18(3):233–8.
- [16] Li G, Cheung R, Ma Q, Yang E. Visual cortical activations on fMRI upon stimulation of the vision-implicated acupoints. *Neuro-Report* 2003;14(5):669–73.
- [17] Li G, Huang L, Cheung R, Liu S, Ma Q, Yang E. Cortical activations upon stimulation of the sensorimotor-implicated acupoints. *Magn Reson Imaging* 2004;22(5):639–44.
- [18] Chen X, Han J. All three types of opioid receptors in the spinal cord are important for 2/15 Hz electroacupuncture analgesia. *Eur J Pharmacol* 1992;211(2):203–10.
- [19] Wu M, Hsieh J, Xiong J, Yang C, Pan H, Chen Y. Central nervous pathway for acupuncture stimulation: localization of processing with functional MR imaging of the brain—preliminary experience. *Radiology* 1999;212(1):133–41.
- [20] Wu MT, Sheen JM, Chuang KH, Yang P, Chin SL, Tsai CY, et al. Neuronal specificity of acupuncture response: a fMRI study with electroacupuncture. *Neuroimage* 2002;16(4):1028–37.
- [21] Cho Z, Chung S, Jones J, Park J, Park H, Lee H. New findings of the correlation between acupoints and corresponding brain cortices using functional MRI. *Proc Natl Acad Sci U S A* 1998;95(5): 2670–3.
- [22] Hui KK, Liu J, Makris N, Gollub RL, Chen AJ, Moore CI, et al. Acupuncture modulates the limbic system and subcortical gray structures of the human brain: evidence from fMRI studies in normal subjects. *Hum Brain Mapp* 2000;9(1):13–25.
- [23] Woods RP, Grafton ST, Watson JD, Sicotte NL, Mazziotta JC. Automated Image Registration: II. Intersubject validation of linear and nonlinear models. *J Comput Assist Tomogr* 1998; 22(1):153–65.
- [24] Anson BH. The aortic arch and its branches. In: Luisada A, editor. *Cardiology*. New York: McGraw-Hill; 1963. p. 119.

- [25] Friston KJ, Zeigler P, Turner R. Analysis of functional MRI time-series. *Hum Brain Mapping* 1994;1:153–71.
- [26] Hsieh J, Tu C, Chen F, Chen M, Yeh T, Cheng H. Activation of the hypothalamus characterizes the acupuncture stimulation at the analgesic point in human: a positron emission tomography study. *Neurosci Lett* 2001;307(2):105–8.
- [27] Siedentopf CM, Golaszewski SM, Mottaghy FM, Ruff CC, Felber S, Schlager A. Functional magnetic resonance imaging detects activation of the visual association cortex during laser acupuncture of the foot in humans. *Neurosci Lett* 2002;327(1):53–6.
- [28] Biella G, Sotgiu M, Pellegata G, Paulesu E, Castiglioni I, Fazio F. Acupuncture produces central activations in pain regions. *Neuroimage* 2001;14(1):60–6.
- [29] Yoshizawa T, Nose T, Moore G, Sillerud L. Functional magnetic resonance imaging of motor activation in the human cervical spinal cord. *Neuroimage* 1996;4:174–82.
- [30] Stroman PW, Kornelsen J, Lawrence J. An improved method for spinal functional MRI with large volume coverage of the spinal cord. *J Magn Reson Imaging* 2005;21(5):520–6.
- [31] Stroman PW, Krause V, Maliszka KL, Frankenstein UN, Tomanek B. Functional magnetic resonance imaging of the human cervical spinal cord with stimulation of different sensory dermatomes. *Magn Reson Imaging* 2002;20(1):1–6.
- [32] Stroman PW, Ryner LN. Functional MRI of motor and sensory activation in the human spinal cord. *Magn Reson Imaging* 2001;19(1):27–32.